**JOURNAL OF THEORETICAL AND APPLIED MECHANICS**
**45**, 4, pp. 785-800, Warsaw 2007

# INVESTIGATION OF UNSTEADY VORTICITY LAYER ERUPTION INDUCED BY VORTEX PATCH USING VORTEX PARTICLES METHOD

Henryk Kudela
Ziemowit Miłosz Malecha

*Politechnika Wrocławska, Instytut Techniki Cieplnej i Mechaniki Płynów, Wrocław, Poland*
*e-mail: henryk.kudela@pwr.wroc.pl; ziemowit.malecha@pwr.wroc.pl*

The study of eruption of the vortex boundary layer phenomenon due to motion of the patch of vorticity above the wall is presented here. The vortex particle method is chosen to investigate the phenomenon. It shows the eruptive character of the vortex induced boundary layer. Such visualization is possible through the use of the vortex particle method. Description of the numerical method is given. The obtained numerical results are confronted with the numerical and analytical data of other researchers, conforming to a great extent with the conclusions.

*Key words*: vortex method, eruption, boundary layer

## 1. Introduction

The loss of stability in the boundary layer, which manifests itself in a sudden eruption and injection of a fluid particle from a solid wall layer to the flow interior, is a very interesting hydrodynamical phenomenon with great practical significance (Sengupta *et al.*, 2002; Sengupta and Sarkar, 2003; Smith and Walker, 1996). It occurs during turbine blades motion, where the ejected fluid generates wake, which affects other blades. Eruption of the wall vortex layer on an airfoil profile initiates the "dynamic stall" phenomena that influence the lift force and can seriously affect steerability (Ekaterinaris and Platzer, 1997). The eruption influences the mixing and heat exchange.

It is well known that the wall is the only source of the vorticity. Recognition of the mechanism by which the vorticity is introduced to the interior of the flow has a fundamental meaning for understanding of the transition to turbulence

and turbulent boundary layer behavior (Sengupta *et al.*, 2002; Smith and Walker, 1996). The vorticity, which is created on a rigid wall, diffuses to the flow domain. However, if the fluid viscosity is low enough, the vorticity is concentrated in a small zone along the wall. In the presence of the external vortex structure, this vorticity may be violently ejected into the outer flow. It changes flow conditions. The key to explain why such an eruption takes place lies in appreciation of the nature of a viscous response near the wall to the flow induced by the vortex patch passing in an otherwise stagnant flow above the wall (Doligalski, 1994; Peridier *et al.*, 1991a,b; Van Dommelen and Cowley, 1990).

In order to visualize and study the whole process of the eruption of the vortex layer described above, we use the vortex particle methods. The computations are carried out in Lagrangian variables. The study of the evolution of vorticity is done by tracing the position of vortex particles. Results and conclusions are worked out on the basis of velocity, energy and vorticity analysis.

## 2. Equations of fluid motion

Equations of viscous and incompressible fluid motion in a two-dimensional space have the following form

$$\frac{\partial u}{\partial t} + (\boldsymbol{u} \cdot \nabla)\boldsymbol{u} = -\frac{1}{\rho}\nabla p + \nu \Delta \boldsymbol{u} \qquad \frac{\partial u_1}{\partial x} + \frac{\partial u_2}{\partial y} = 0 \tag{2.1}$$

where $\boldsymbol{u} = [u_1, u_2]$ is the velocity vector, $\rho$ – fluid density, $\nu$ – coefficient of kinematic viscosity, $p$ – pressure, $\nabla = (\partial^2/\partial x^2) + (\partial^2/\partial y^2)$ – Laplace's operator.

It is assumed that density is constant, so it can be put under the pressure gradient operator. Equations (2.1) must be completed with initial and boundary conditions

$$\begin{aligned} &\boldsymbol{u} = \boldsymbol{0} \qquad \text{dla} \quad (x,y) \in \partial\Omega \\ &\boldsymbol{u}(\boldsymbol{x}, 0) = \boldsymbol{u}_0(x,y) \end{aligned} \tag{2.2}$$

where $\partial\Omega$ means the solid wall and $\boldsymbol{u}_0(x,y)$ means the initial velocity. In our case, this initial velocity is the velocity induced by the vortex patch. Equation $(2.1)_2$, which expresses the incompressibility of fluid, ensures the existence of a stream function $\psi$, so that $u_1 = \psi_y$, $u_2 = -\psi_x$. In the two dimensional

space, the vorticity vector $\mathrm{rot}\,(\boldsymbol{u}) = k\omega = \partial_x u_2 - \partial_y u_1$ has only one non-zero component, where $k$ means a unit vector orthogonal to the plane of motion. Applying the rot$(\cdot)$ operator to both sides of equation $(2.1)_1$, it can be transformed into the Helmholtz equation, which describes the evolution of vorticity in time

$$\omega_t + u_1\omega_x + u_2\omega_y = \nu\Delta\omega \tag{2.3}$$

where

$$\Delta\psi = -\omega \qquad u_1 = \partial_y\psi \qquad u_2 = -\partial_x\psi \tag{2.4}$$

In that way, vectorial equation $(2.1)_1$ is replaced by scalar equation (2.5) for $\omega(x, y, t)$. It is worth noticing that now we do not have the pressure term in this equation. Usually, in the vortex method, the viscous splitting algorithm is used (Cottet and Koumoutsakos, 2000). Equation (2.3) is solved in two steps: at first, the inviscid equation is solved

$$\omega_t + u_1\omega_x + u_2\omega_y = 0 \tag{2.5}$$

and then, the diffusion equation (Stokes problem)

$$\omega_t = \nu\Delta\omega \tag{2.6}$$

is solved. For solving equation (2.5), the vortex particles method is used.

## 3. Description of the vortex particles method

From equation (2.5), it results that the vorticity is conserved along the particle path. Hence $\omega(\boldsymbol{x}(t, \boldsymbol{\alpha}), t) = \omega(\boldsymbol{\alpha}, 0)$. From the third Helmholtz theorem (Wu *et al.*, 2006), we know that vorticity lines move with the fluid. It means that motion of vortex particles is described by the differential equation

$$\frac{d\boldsymbol{x}_p}{dt} = \boldsymbol{u}(\boldsymbol{x}_p, t) \qquad \boldsymbol{x}(0, \boldsymbol{\alpha}) = \boldsymbol{\alpha} \tag{3.1}$$

where $\boldsymbol{\alpha} = (\alpha_1, \alpha_2)$ are Lagrangian coordinates of the fluid particle. On account of equation (2.4), the velocity can be determined from the vorticity distribution by convolution of the Green function $K$ and $\omega$ (Hald, 1991; Wu *et al.*, 2006)

$$\boldsymbol{u}(\boldsymbol{x}) = \int K(\boldsymbol{x} - \boldsymbol{x}')\omega(\boldsymbol{x}', t)\, d\boldsymbol{x}' \tag{3.2}$$

where

$$K(\boldsymbol{x}) = \frac{1}{2\pi|\boldsymbol{x}|}(y,x) \qquad |\boldsymbol{x}| = \sqrt{x^2+y^2}$$

Equation (3.2) is a fundamental formula in the direct summation vortex method (Kudela, 1995), but the velocity of vortex particles can be found by solving the Poisson equation for stream function (2.4) by using the finite difference method and then interpolating from the grid note to the position of the vortex particles. This approach dramatically speed-up calculations, and just that approach is used in this work (Cottet and Koumoutsakos, 2000; Kudela, 1995).

In numerical calculations, we have to replace the infinite set of differential equations (3.1) by a finite one. The $\boldsymbol{\alpha}$-space (Lagrangian variable) is covered by a regular grid $(j_1\Delta x, j_2\Delta y)$ $(j_1, j_2 = 1, \ldots, N)$, $\Delta x = \Delta y = h$. This grid is also used later for solving the Poisson equation for the stream function. The initial vorticity field is replaced by particle distribution of point vortices. Each particle has mass (circulation)

$$\Gamma_p = \int\limits_{A_p} \omega(x,y)\, dA \approx h^2\overline{\omega} \tag{3.3}$$

where $A_p = h^2$ means the area of the $p$th cell and $\overline{\omega}$ is the average vorticity in the cell. The vorticity is approximated by a sum of delta Dirac measures

$$\omega(\boldsymbol{x}) \approx \sum_{i=1}^{N} \Gamma_p \delta(\boldsymbol{x} - \boldsymbol{x}_p) \tag{3.4}$$

where $N$ is the number of particles and $\delta$ means the Dirac delta function, $\boldsymbol{x} = (x,y)$. The circulations of particles are constant in time.

The solution to equation (2.5) in the interval $(t_n, t_{n+1})$ is obtained by solving the system of differential equations

$$\frac{d\boldsymbol{x}_p(t)}{dt} = \boldsymbol{u}(\boldsymbol{x}_p^n(t), t) \qquad \boldsymbol{x}_p(t_n) = \boldsymbol{x}_p^n \qquad \begin{matrix} t_n \leqslant t \leqslant t_{n+1} \\ p = 1, \ldots, N \end{matrix} \tag{3.5}$$

and a new position of particles becomes an approximate solution to (2.5) at the instant $t = t^{n+1}$

$$\omega^{n+1}(\boldsymbol{x}) = \sum_{p=1}^{N} \Gamma_p(\boldsymbol{x} - \boldsymbol{x}_p^{n+1}) \qquad \boldsymbol{x}_p^{n+1} = \boldsymbol{x}_p(t_{n+1}) \tag{3.6}$$

The fluid velocity is calculated from the stream function by solving Poisson equation (2.4) on the grid, and its values from the grid nodes are interpolated to the position of particles.

To solve diffusion equation (2.6), we use a stochastic (random) method. In context of Helmholtz equation (2.3), this has an interesting motivation (Long, 1988). The generalization of particle paths $\boldsymbol{x}_p(t)$ (Eq. (3.5)) for viscous equation (2.3) is a diffusion process $\boldsymbol{X}(t,\boldsymbol{\alpha})$, $t>0$ defined by the stochastic differential equation (Hald, 1991; Kloeden and Platen, 1995; Long, 1988)

$$d\boldsymbol{X}(t,\boldsymbol{\alpha}) = \boldsymbol{u}(\boldsymbol{X}(t,\boldsymbol{\alpha}),t)\,dt + \sqrt{2\nu}\,d\boldsymbol{W}(t) \qquad \boldsymbol{X}(\boldsymbol{\alpha},0)=\boldsymbol{\alpha} \tag{3.7}$$

where $\boldsymbol{W}(t)$ is a Brownian motion in $\mathbb{R}^2$ (standard Wiener process). One may notice that for $\nu=0$, we obtain a trajectory of inviscid motion given by (3.5). Each sample path of Brownian motion $\boldsymbol{W}(t)$ is a continuous and nowhere differentiable function with $\boldsymbol{W}(0)=\boldsymbol{0}$ (Kloeden and Platen, 1995). An infinite number of particles moving along their trajectories given by (3.7), describes motion of the viscous fluid.

Let $G(\boldsymbol{x},t;\boldsymbol{\alpha},s)$ means the transition probability density that the particle reaches the position $\boldsymbol{x}$ at the time $t$ from the position $\boldsymbol{\alpha}$ and time $s<t$. In the terminology of stochastic processes, we know that the function $G(\boldsymbol{x},t;\boldsymbol{\alpha},s)$ satisfies the Fokker-Planck-Kolgomorov (F-P-K) equation (Kloeden and Platen, 1995; Sobczyk, 1996). Since $\nabla\cdot\omega=0$, equation (2.3) can be transformed into a form that is identical to the F-P-K equation

$$\frac{\partial\omega}{\partial t} + \nabla\cdot(\omega\boldsymbol{u}) = \nu\Delta\omega \tag{3.8}$$

The solution $\boldsymbol{X}(t,\boldsymbol{\alpha})$ to stochastic equation (3.7) expresses the position of a particle that has the value $\omega(\boldsymbol{X}(t,\boldsymbol{\alpha}),t)$ and which at the moment $t=0$ was in $\boldsymbol{\alpha}$. Vorticity $\omega(\boldsymbol{x},t)$ can be interpreted as the transition probability density.

Let us assume that we reach the time $t=t_n$. Let us take the finite set of $\boldsymbol{\alpha}=\boldsymbol{x}_p$ values. We replace the infinite set of stochastic equations (3.7) by a finite one

$$d\boldsymbol{X}(\boldsymbol{x}_p,t) = \boldsymbol{u}(\boldsymbol{x}_p,t)\;dt + \sqrt{2\nu}\,d\boldsymbol{W}(\boldsymbol{x}_p,t) \qquad p=1,\ldots,N \tag{3.9}$$

To solve (3.8) numerically, we must discretize it in time. Each component of $\boldsymbol{W}(t+\Delta t)-\boldsymbol{W}(t)$ is a Gaussian random variable with the zero mean value and variance $\Delta t$ (Kloeden and Platen, 1995). We choose the improved Euler scheme for stochastic equation (3.9) (Kloeden and Platen, 1995)

$$\begin{aligned}
\boldsymbol{x}_p^* &= \boldsymbol{x}_p^n + \Delta t\boldsymbol{u}^n(\boldsymbol{x}_p) + \sqrt{2\nu\Delta t}\boldsymbol{N}_p \\
\boldsymbol{x}_p^{n+1} &= \boldsymbol{x}_p^n + \frac{1}{2}(\boldsymbol{u}^n(\boldsymbol{x}_p)+\boldsymbol{u}^n(\boldsymbol{x}_p^*))\Delta t + \sqrt{2\nu\Delta t}\boldsymbol{N}_p
\end{aligned} \tag{3.10}$$

where $\boldsymbol{u}(\boldsymbol{x}_p)$ is the velocity interpolated from the grid nodes to the particle positions and $\boldsymbol{N}_p$ is the Gaussian distributed vector $(\boldsymbol{N}_p^1, \boldsymbol{N}_p^2)$ with the zero mean value and a unit variance. This vector can be obtained by the Box-Muller method (Kloeden and Platen, 1995)

$$N^{(1)} = \cos(2\pi U^{(1)})\sqrt{-2\ln U^{(2)}} \qquad N^{(2)} = \sin(2\pi U^{(1)})\sqrt{-2\ln U^{(2)}} \tag{3.11}$$

where $U^{(1)}$ and $U^{(2)}$ are independent random variables uniformly distributed in $[0,1]$. We must note that we are not forced to use the random walk method for solving the diffusion equation. This method is fast and easy in realization, but one can try simulating the viscous effect of the fluid by a deterministic method (Cottet and Koumoutsakos, 2000).

The essential part of calculations is the redistribution of the particles circulation to the grid nodes to obtain the vorticity there. We need this for solving the Poisson equation for stream function (2.4). The redistribution can be done by an area-weighting scheme as follows

$$\omega_j = \frac{1}{A_i}\sum_p \Gamma_p \varphi_j(\boldsymbol{x}_p) \tag{3.12}$$

where summation includes particles which are inside the support function $\varphi_j$. The index $j$ means the $j$th node $j = (j_1\Delta x, j_2\Delta y)$. As the function $\varphi$, the first order B-function is taken

$$\varphi(\boldsymbol{x}) = \begin{cases} 1-|\boldsymbol{x}| & \text{for} \quad |\boldsymbol{x}| < 1 \\ 0 & \text{for} \quad |\boldsymbol{x}| \geqslant 1 \end{cases} \tag{3.13}$$

It can be shown that the redistibution process is conservative and stable in the $L^2$ sense (Cottet and Koumoutsakos, 2000). It means that

$$\sum_j h^2\omega_j = \sum_p h^2\omega(\boldsymbol{x}_p) \qquad \text{and} \qquad \sum_j h^2|\omega_j|^2 \leqslant \sum_p h^2|\omega(\boldsymbol{x}_p)|^2$$

The second important step of calculations is the interpolation of the velocity field to the particles location. The velocity interpolated to the position of particles may be expressed as follows

$$\boldsymbol{u}(\boldsymbol{x}_p) = \sum_j \boldsymbol{u}_j l_h(\boldsymbol{x}_p - \boldsymbol{x}_j) \tag{3.14}$$

where $l_h$ is the base function of the bilinear Lagrange function.

## 4. Realisation of the boundary condition on a solid wall

Condition $(2.2)_1$ for the viscous fluid flow means no slip of the fluid at the wall. Both normal and tangent components of the velocity to the wall should equal zero. Description of the flow using the vorticity and stream function by removing from the equation the pressure term made the equations easier but caused complications in the realization of no-slip condition $(2.2)_1$. When using the vortex methods, condition $(2.2)_1$ is realized by generation of the proper vorticity amount on the wall (Cottet and Koumoutsakos, 2000; Kudela, 1995). It can be achieved by choosing an appropriate value of the vorticity or the vorticity flux $\nu(\partial\omega/\partial n)$ (Koumoutsakos *et al.*, 1994). In this study, the second approach is chosen. For Euler's equation, the distribution of the vorticity inside of the flow domain generates non-zero tangent velocity at the wall $u_s$. This tangent velocity can be regarded as a vortex layer, which is established along the rigid boundary with the intensity $\gamma = u_s$. To understand how the vorticity flux can eliminate the undesirable tangent component of velocity, let us consider equation $(2.1)_1$ at the wall

$$\left.\frac{du}{dt}\right|_{wall} = -\left.\frac{\partial p}{\partial x}\right|_{wall} - \nu\left.\frac{\partial \omega}{\partial y}\right|_{wall} \tag{4.1}$$

where $(x, y)$ means a variable coordinate tangent and normal to the wall. It can be noticed that the acceleration is connected with the pressure gradient and vorticity flux. When an additional non-zero tangent velocity appears at the wall, it may be interpreted as an additional acceleration which appears at the wall in a short time $\Delta t$. This acceleration has to be compensated by the additional vorticity flux $\nu(\partial\omega/\partial y)$. So, one can write

$$\frac{u^{n+1} - u^n}{\Delta t} \approx \nu\frac{\partial \omega}{\partial y} \tag{4.2}$$

If the tangent velocity which appears on the wall in the interval $\Delta t$, then the velocity is equal to $u_s = \nu\Delta t\partial\omega/\partial y$. To compensate this velocity to zero, one must change the sign of $u_s$, Thus the normal derivative of the vorticity will be

$$\frac{\partial \omega}{\partial n} = -\frac{u_s}{\nu\Delta t} \tag{4.3}$$

To introduce an additional vorticity to the flow domain, which diffuses from the wall, the diffusion equation is solved

$$\omega_t = \nu\Delta\omega \qquad \omega(x, y, 0) = 0 \qquad \frac{\partial \omega}{\partial n} = -\frac{u_s}{\nu\delta t} \tag{4.4}$$

It can be noticed that the initial condition for vorticity is equal to zero. The vorticity field achieved from the solution to equations (4.4) is replaced by vortex particles in grid nodes according to formula (3.3). The vorticity that diffused to the domain from the wall is different from zero only on the wall and on a few grids near the wall. The vortex particles which drop out from the domain during the solution of stochastic equation are eliminated from calculations.

## 5. Numerical calculations

In Fig. 1, a sketch of the computational domain and the initial vortex patch arre shown. The calculation starts when the fluid is at rest. The size of the computational domain is chosen by a trail and error method in such a way as to reduce the influence of the boundary conditions. Dimensions of the domain are: length $L = 10$ and height $H = 10$. The boundary condition for the stream function is assumed periodic in $x$ and zero for the upper $(y = 10)$ and lower $(y = 0)$ boundary. The initial position of the patch is $x_0 = 7.2$, $y_0 = 0.6$. The initial radius of the patch is $r = 0.1$ and its vorticity $\omega_0 = -4$. One can estimate that the module of the velocity induced by the patch on the upper boundary of the domain equals $\Gamma/2\pi H \approx 0.002$, where $\Gamma = \pi r^r 2\omega_0$. So the influence of the upper boundary condition on the behavior of the vortex layer along the solid wall seems to be small. We checked this experimentally by repeating the calculation in a twice smaller domain. The results are nearly the same. The size of the mesh and the time step are $\Delta x = \Delta y = 0.02$, $\Delta t = 0.02$. The patch is replaced by $N = 121$ vortex particles.

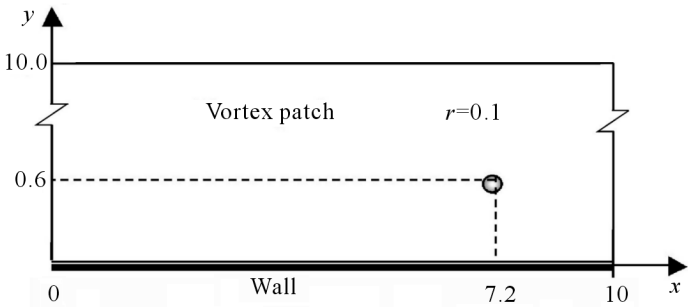


Fig. 1. Computation area of the investigated problem (the scale is not conserved)

One computational time step from $t_n$ to $t_n + \Delta t$ runs as follows:

1. Redistribution of the vortex circulation to the mesh nodes (Eq. (3.12))
2. Solution to the Poisson equation for the stream function

$$\begin{aligned} &\Delta\psi = -\omega \\ &\psi\Big|_{x=0} = \psi\Big|_{x=L} \qquad\qquad \psi\Big|_{y=0} = \psi\Big|_{y=H} = 0 \end{aligned} \tag{5.1}$$

3. Calculation of the velocity in grid nodes

$$\begin{aligned} u_{i,j} &= \frac{\psi(x_i, y_j + \Delta y) - \psi(x_i, y_j - \Delta y)}{2\Delta y} \\ v_{i,j} &= -\frac{\psi(x_i + \Delta x, y) - \psi(x_i - \Delta x, y_j)}{2\Delta x} \end{aligned} \tag{5.2}$$

4. Calculation of the vorticity layer $\gamma = u_s$, solution to diffusion problem (4.4) and introduction of the new vortex particles.
5. Movement of particles according to stochastic differential equation (3.9).

To solve (5.1), a fast elliptic solver was used. This solver was also adopted to solve diffusion equation (4.4). Replacing the time derivative by $\omega_t|_{t=t^{n+1}} \approx \omega^{n+1}/\Delta t$ $(\omega^n = 0)$, one obtains the elliptic problem

$$\begin{aligned} &\Delta\omega^{n+1} - \frac{\omega^{n+1}}{\nu\Delta t} = 0 \\ &\frac{\partial\omega}{\partial y}\Big|_{y=0} = -\frac{u_s}{\Delta t\nu} \qquad\qquad \omega\Big|_{x=0} = \omega\Big|_{x=L} \qquad\qquad \omega\Big|_{y=H} = 0 \end{aligned} \tag{5.3}$$

To interpolate velocity from the mesh nodes to the location of particles, the bilinear Lagrange interpolation was used (formula (3.6)).

## 6. Numerical results

The eruption phenomenon can be understood by investigating the effect of viscosity on fluid motion close to the wall and just under the vortex patch. The vortex patch due to presence of the wall moves along the wall from right to left. The direction of motion is determined by the sign of the vorticity carried

by the patch. The vortex patch, due to its small support, can be treated approximately as a point vortex. The vortex patch generates an unsteady boundary layer. The maximum velocity induced by the patch is exactly under it. And at this place, the pressure has the minimal value. In front of the patch, the velocity decreases and pressure increases. That is why the pressure gradient is adverse to the direction of patch motion. Such a pressure gradient slows down motion of the fluid, brings on stagnation points in velocity and a small recirculation zone, like a bubble. This bubble grows perpendicularly to the wall and finally leads to eruption in that direction. Figure 2 shows stream lines in the vicinity of the eruption place, which results from the analytical investigation presented by Doligalski (1994), Peridier *et al.* (1991a), Smith and Walker (1996), Van Dommelen and Cowley (1990). Region number I presents a viscous boundary layer under the vortex patch. In region number II, the flow direction is opposite to the main flow and it is regarded as free from the vorticity (Doligalski, 1994). This region separates the boundary layer from two different regions I and III, is very dynamic and controls the eruption (Doligalski, 1994; Peridier *et al.*, 1991a,b).

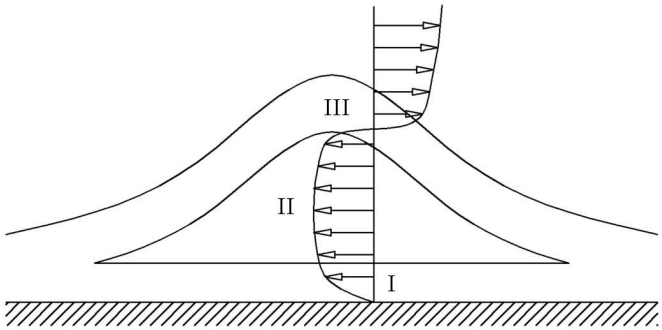


Fig. 2. Instantaneous boundary layer region near the point of eruption

Figure 3 presents the sequence of time evolution of stream lines during vortex patch motion. For $t = 20$, the occurence of the recirculation zone can be noticed. For $t = 32$, the recirculation region increases and pushes away fluid elements from the wall. One can notice concentration of the stream lines. It means a very high velocity gradient along that lines. Within the interval $t = 44$ and $t = 50$, the beginning of the next recirculation zone is seen. The boundary layer eruption process is clearly seen in Fig. 4, which shows a sequence of the vorticity evolution. The frames correspond to Fig. 3. The eruption phenomenon manifests itself here as an explosion of the concentrated vorticity jet, and creation of the secondary vortex structure. The necessary eruption condition

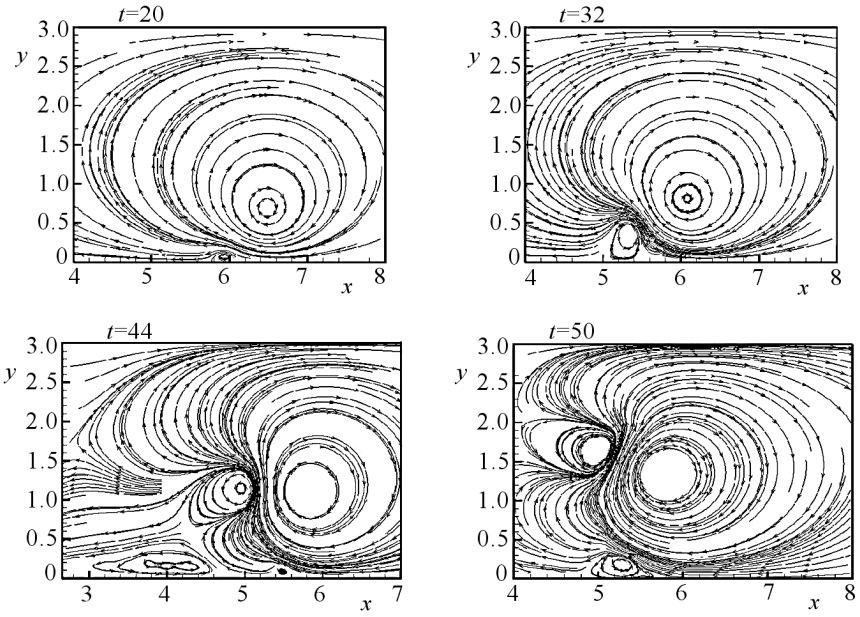


Fig. 3. Sequence of time frames for the stream lines

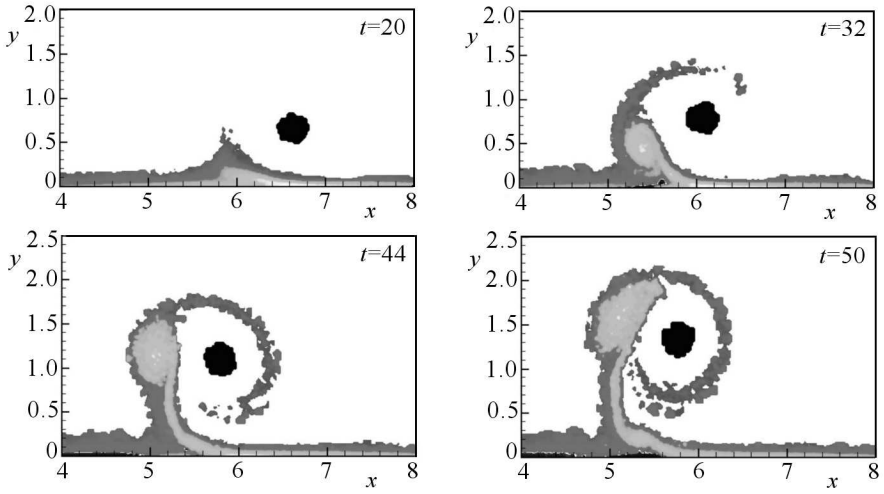


Fig. 4. Time frames of the vorticity. The vortex patch interaction with wall, $\omega_0 = -4$, $\nu = 0.00002$

is a low viscosity value. If the viscosity is high enough, the vorticity can not concentrate and diffuses quickly from the wall. The recirculation region, which is established inside the boundary layer, is caused by the viscosity effect and initiates the eruption. The vorticity which is thrown out to the flow domain significantly changes motion of the primary vortex.

Kinetic energy $E_k = u_1^2 + u_2^2$ of the flow was also examined. As expected, the eruption starts in the place where the kinetic energy was minimal. Figure 5 shows the evolution of the kinetic energy around moving vortex patch. The dark region in the boundary layer corresponds to the energy minimum. Here, the velocity is minimal as well, and this causes vorticity concentration.

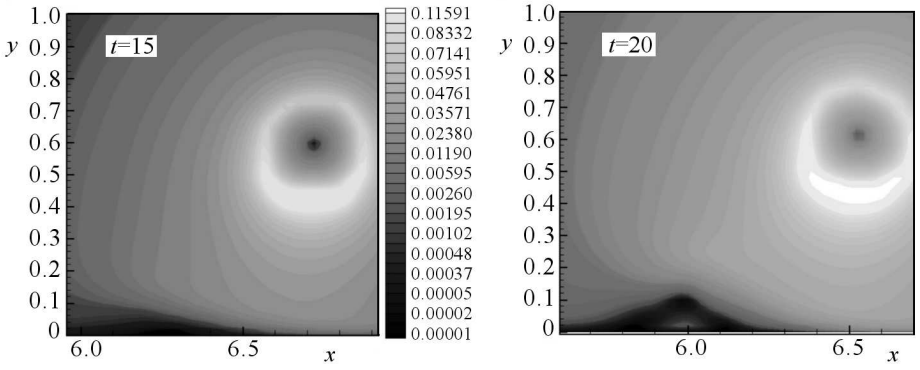


Fig. 5. Isolines of kinetic energy for $t = 15$ and $t = 20$. The appearance of the recirculation zone is visible where the kinetic energy is zero

In many papers (Peridier *et al.*, 1991a; Smith and Walker, 1996; Van Dommelen and Cowley, 1990) concerning the eruption phenomenon, it is emphasized that the eruption effect is accompanied by the zero vorticity line $\omega = 0$. This line is seen in Fig. 6 as a border line between positive and negative values of the vorticity in the boundary layer. For better illustration, Fig. 6 incorporates the zebra technique (each vorticity range is separated by a black lane).

In Table 1, numerical results for different intensities of the primary vortex patch are set together and compared. The first column shows the primary vortex intensity. The second column shows the intensity of the secondary vortex. In the third column, distance covered by the vortex patch to the beginning of the eruption is given. The fourth one shows time after which the eruption takes place. The results suggest that the intensity of the secondary vortex, which blows off from the wall, is about 50 percent of the primary vortex intensity. Obviously, the primary vortex patch circulation has the opposite sign to the secondary vortex. Interestingly, the separation always occurs almost in

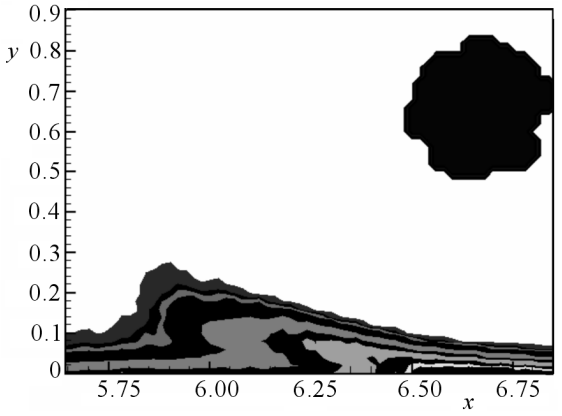


Fig. 6. Blow-up of vorticity isolines in the vorticity layer around the eruption point. The white lane near the point $x = 6.5$ means $\omega = 0$

the same place but in a different time. Figure 7 presents the flow region which corresponds to the sketch shown in Fig. 1. The first frame shows the vorticity field, the second one – velocity field. On the first frame, the appearance of the secondary vortex structure is clearly seen. The second frame shows that in critical zone III, the $x$ velocity component equals zero and the middle of this zone corresponds to the secondary vortex center.

**Table 1.** Calculation results

| Primary vortex structure intensity | Secondary vortex structure intensity | Eruption start | |
|---|---|---|---|
| | | distance | time |
| −1 | 0.47 | 0.85 | 41.6 |
| −2 | 0.88 | 0.9 | 24.1 |
| −4 | 1.76 | 0.9 | 15 |
| −8 | 4.16 | 0.945 | 8 |

## 7. Conclusions

Based on the presented results, it is evident that the eruption of the vortex layer form the wall is an effect of the interaction of the vorticity diffused from the wall and the external interaction with the vortex patch. It is shown that the eruption vortex boundary layer manifested itself by ejection of a narrow stream of vorticity from the wall to the external flow. The initiation of the

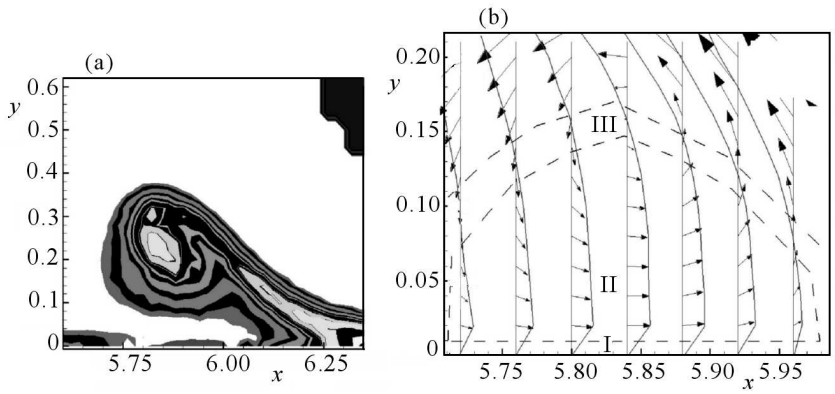


Fig. 7. Blow-up of the space around the eruption point: (a) secondary vortex (a fragment of the primary vortex patch is visible in the upper right corner), (b) velocity field with marked zones I, II, III (as in Fig. 2

eruption process starts with formation of a small recirculating eddy inside of the vortex boundary layer. It is regarded that the zero vorticity line within the vortex layer heralds a subsequent eruption (Smith and Walker, 1996; Van Dommelen and Cowley, 1990).

All these facts were predicted by theoretical considerations (Doligalski, 1994; Peridier *et al.*, 1991a,b; Smith and Walker, 1996; Van Dommelen and Cowley, 1990). The use of the vortex particle method made it possible to clearly show these phenomena. It stems from the fact that the calculations were carried out in Lagrangian variables and all essential elements of the phenomena like generation and diffusion of the vorticity from the wall as well as its interaction with the vortex patch were directly incorporated into the calculation.

## Symbols

$u_1, u_2$ – $x$ and $y$ component of velocity, respectively
$\omega_0$ – vorticity of vortex patch
$\omega$ – z-component of vorticity field
$\psi$ – stream function

## Subscripts and superscripts

$x, y, t$ – differentation with respect to $x$, $y$ and time

## References


1. COTTET G.-H., KOUMOUTRAKOS P.D., 2000, *Vortex Methods: Theory and Practice*, Cambridge Univ. Press
2. DOLIGALSKI T.L., 1994, Vortex interactions with walls, *Ann. Rev. Fluid Mech.*, **26**, 573-616
3. EKATERINARIS J., PLATZER M., 1997, Computational prediction of airfoil dynamic stall, *Porg. Aerpspace Sci.*, **33**, 759-846
4. HALD O.H., 1991, Convergnce of vortex methods, In: *Vortex Methods and Vortex Motion*, K.E. Gustawson, J.A. Sethian (Edit.), SIAM
5. KLOEDEN P.E., PLATEN E., 1995, *Numerical Solution of Stochastic Differential Equations*, Springer
6. KOUMOUTSAKOS P., LEONARD A., PEPIN F., 1994, Boundary condition for viscous vortex methods, *J. of Computational Physics*, **113**, 52-61
7. KUDELA H., 1995, *Modelowanie zjawisk hydrodynamicznych metodami dyskretnych wirów*, Oficyna Wydawnicza Politechniki Wrocławskiej, Wrocław
8. KUDELA H., 1999, Application of the vortex-in-cell method for the simulation of the two-dimensional viscous flow, *Task Quarterly*, **3**, 3, 343-360
9. LONG D.-G., 1988, Convergence of the random vortex method in two dimensions, *J. Amer. Mathem. Society*, **1**, 4, 779-804
10. PERIDIER V.J., SMITH F.T., WALKER J.D.A., 1991a, Vortex-induced boundary-layer separation. Part 1. The unsteady limit problem $\mathrm{Re} \to \infty$, *J. Fluid Mech.*, **232**, 99-131
11. PERIDIER V.J., SMITH F.T., WALKER J.D.A., 1991b, Vortex-induced boundary-layer separation. Part 2. Unsteady interacting boundary-layer theory, *J. Fluid Mech.*, **232**, 133-165
12. SENGUPTA T.K., SARKAR S., DE S., 2003, Vortex-induced instability of incompressible wall-bounded shear layer, *J. Fluid Mech.*, **493**, 277-286
13. SENGUPTA T.K., CHATTOPADHYAY M., WANG Z.Y., YEO K.S., 2002, Bypass mechanism of transition to turbulence, *J. of Fluids and Structures*, **16**, 1, 15-29
14. SMITH C.R, WALKER D.A., 1996, Turbulent wall-layer vorticies, In: *Fluid Vorices*, S.I. Green (Edit.), Kluwer, 235-290
15. SOBCZYK K., 1996, *Stochastyczne równania różniczkowe*, Wydawnictwo Naukowo-Techniczne, Warszawa
16. VAN DOMMELEN L.L., COWLEY J.J., 1990, On the Lagrangian description of unsteady boundary layer separation, *J. Fluid Mech.*, **210**, 593-626
17. WU J.-Z., MA H.-Y., ZHOU M.-D., 2006, *Vorticity and Vortex Dynamics*, Springer

## Badanie zjawiska niestacjonarnej erupcji warstwy wirowej wywołanej łatą wirową metodą cząstek wirowych

Streszczenie

W pracy przedstawiono wyniki badań numerycznych zjawiska erupcji warstwy wirowej wywołanej przejściem skoncentrowanej struktury wirowej w pobliżu ściany. Do badań wybrano metodę cząstek wirowych. Pokazano erupcyjny charakter warstwy przyściennej indukowanej przez łatę wirową. Przedstawiono dokładny opis prezentowanej metody numerycznej. Omówiono mechanizm formowania się osobliwości w warstwie przyściennej. Wyniki numeryczne skonfrontowano z wynikami badań analityczno-numerycznymi innych badaczy. Przedstawione wyniki numeryczne dobrze potwierdziły hipotezy dotyczące natury erupcji warstwy. Zweryfikowały tym samym niezwykłą przydatność do badania tego typu zjawisk metody cząstek wirowych.

*Manuscript received January 18, 2007; accepted May 23, 2007*